Diffusional dynamics of an active rhodamine-labeled 1,4-dihydropyridine in sarcolemmal lipid multibilayers

R. Preston Mason and David W. Chester
Departments of Radiology and Biochemistry, and the Biomolecular Structure Analysis Center
University of Connecticut Health Center, Farmington, Connecticut 06032

ABSTRACT A "membrane bilayer pathway" model, involving ligand partition into the bilayer, lateral diffusion, and receptor binding has been invoked to describe the 1,4-dihydropyridine (DHP) calcium channel antagonist receptor binding mechanism. In an earlier study (Chester et al. 1987. *Biophys. J.* 52:1021–1030), the diffusional component of this model was examined using an active fluorescence labeled DHP calcium channel antagonist, nisoldipine-lissamine rhodamine B (Ns-R), in purified cardiac sarcolemmal (CSL) lipid multibilayers. Diffusion coefficient measurements on membrane-bound drug and phospholipid at maximum bilayer hydration yielded similar values (3.8×10^{-8} cm^2/s). However, decreases in bilayer hydration resulted in dramatically reduced diffusion coefficient values for both probes with substantially greater impact on Ns-R diffusion. These data suggested that hydration dependent diffusional differences could be a funciton of relative probe location along the bilayer normal. In this communication, we have addressed the relative effect of the rhodamine substituent on Ns-R diffusion complex by examining the diffusional dynamics of free rhodamine B under the same conditions used to evaluate Ns-R complex and phospholipid diffusion. X-ray diffraction studies were performed to determine the Ns-R location in the membrane and model the CSL lipid bilayer profile structure to give a rationale for the differences in probe diffusional dynamics as a function of interbilayer water space.

INTRODUCTION

1,4-Dihydropyridine (DHP) calcium channel antagonists play an important role in the excitation-contraction coupling mechanism of cardiac and smooth muscle by modulating the transmembrane influx of extracellular calcium. DHP calcium channel antagonists bind with high affinity to specific protein receptors in membranes isolated from a variety of tissues (Janis et al., 1987). Since receptor site density in cardiac sarcolemmal membranes is low (Colvin et al., 1985), theoretical consideration of a two-step "membrane bilayer" pathway (vs. a one-step "aqueous" pathway) indicated that this route should yield a substantial rate advantage, particularly when considering highly stereospecific drug–receptor interactions. This membrane model involves drug partition to an energy-favorable position in the bilayer, lateral diffusion within a discrete plane of the bilayer, and subsequent specific receptor binding (Rhodes et al., 1985).

We have identified, using x-ray and neutron diffraction, the location of several DHPs at the hydrocarbon core/water interface in both native and model membranes (Herbette et al., 1986; Mason et al., 1989*b*). This position defines a plane of locally high ligand concentration and is consistent with membrane partition coefficients (K_p) for these drugs which range from 5,000 to 150,000 (Herbette et al., 1986). Similarly, the heterocyclic ring structure of the phenothiazine drug class has been shown by Frenzel and co-workers (1978) to be located just beneath the hydrocarbon core/water interface. As such, there are several lipophilic ligand classes which, owing to the physical chemical nature of the bilayer interface, partition to this same general locale.

Interestingly, Giraudat et al. (1987) have identified a phenothiazine binding domain on one of the hydrophobic spanning domains of the acetylcholine receptor demonstrating that aqueous phase inaccessible sites do exist. In the β receptor system, Kobilka and co-workers (1988) have demonstrated that deleting one of the putative transmembrane spanning segments results in the apparent loss of the receptor antagonist (e.g., propranolol) binding domain. The primary structure of the rabbit skeletal muscle DHP receptor has been deduced from DNA sequence analysis (Tanabe et al., 1987). The polypeptide chain comprises six possible transmembrane helices (Tanabe et al., 1987). These data, while not conclusive proof, support the notion that bilayer partition to some discrete location in the membrane bilayer is an integral first step in the DHP receptor-binding process.

We have recently evaluated the lateral diffusion rate for an active rhodamine-labeled DHP, nisoldipine-lissamine rhodamine (Ns-R), in cardiac sarcolemmal (CSL) lipid multibilayers with the use of fluorescence redistribution after photobleaching (FRAP) (Chester et al., 1987).

0006-3495/89/12/1193/09 $2.00

The multipoint FRAP technique, as described by Koppel (1979), was used to assess the diffusional dynamics of this analogue and the data were compared with phospholipid diffusion. A diffusion coefficient of 3.8×10^{-8} cm^2/s was obtained for both the drug and phospholipid analogues at maximal bilayer hydration. This value is consistent with phospholipid diffusion coefficient measurements in other systems (Eisenger and Halperin, 1986; Vaz et al., 1985; Wu et al., 1977). McCown et al. (1981) demonstrated that decreases in multibilayer hydration state resulted in concomitant decreases in probe diffusion coefficients. They reasoned that the decrease in diffusion was due to surface condensation and steric hindrance effects resulting from dehydration. In our native lipid system, a similar decrease in diffusion coefficient for both Ns-R and phospholipid (I, I'-dihexadecyl-3,3,3',3'-tetramethyl-indocarbanocyanine perchlorate, DiIC$_{16}$) was evident. However, diffusion coefficients for Ns-R and DiIC$_{16}$ diverged substantially as bilayer hydration was decreased. This observation suggested that these probes are located in different regions of the bilayer and lateral diffusion may be differentially affected by intra- and interbilayer forces (hydration, steric, electrostatic, surface condensation, etc.) associated with partial dehydration (Vaz et al., 1986, McCown et al., 1981, McIntosh et al., 1987).

It is the aim of these studies to further examine the bilayer diffusional component (see also Chester et al., 1987) of the "membrane pathway model" for DHP–receptor interactions Rhodes et al., 1985). In our previous communication (Chester et al., 1987), we characterized the diffusion of an active DHP–chromophore complex relative to phospholipid in pure lipid multibilayers. Ns-R molecular size, charge, and potential bilayer location would suggest that the relatively large rhodamine moiety of the Ns-R complex could significantly affect the diffusional dynamics of this ligand in the membrane. Our observation of hydration-dependent differences between Ns-R and phospholipid diffusion (as measured with DiIC$_{16}$) tends to support this notion. Therefore, we have examined separately the diffusional dynamics of free rhodamine compared to the Ns-R complex and phospholipid analogue (DiIC$_{16}$ and *N*-[7-nitrobenz-2-oxa-1,3-diazol-4-yl]palmitoyl-L-α-phosphatidylethanolamine, NBD-PE) to determine the relative effect of the rhodamine moiety on Ns-R diffusion. Secondly, we determined the location of the Ns-R molecule along the bilayer normal and modelled the membrane and interbilayer water space at various relative humidities using low-angle X-ray diffraction. The applied pressure between bilayers as a function of dehydration was calculated using the equation described by McIntosh et al. (1987). These calculations consider the hydration force (resulting from the work required to remove polarized water molecules from between the bilayers) and steric interaction from apposing headgroups which impact strongly on probe diffusion.

The results of this study demonstrate that, under all hydration conditions examined, free rhodamine diffusion is faster than that observed for the Ns-R complex and phospholipid, consistent with diffusion within the interbilayer water space. Structure studies indicate that, as anticipated for this active DHP compound, the rhodamine and DHP moieties of the Ns-R complex are associated with the water space and hydrocarbon core/water interface, respectively. This location is consistent with that observed for other native DHPs (hydrocarbon core/water interface). The observation that Ns-R diffusion is similar to that of phospholipid at maximum bilayer hydration while free rhodamine is yet faster suggests that Ns-R complex diffusion is primarily rate limited by the membrane bound DHP moiety as indicated by the diffraction result. As such, these data suggest that (*a*) the diffusion coefficient obtained for the Ns-R complex at maximal bilayer hydration is a reasonable lower limit for DHP diffusion in bulk lipid, and (*b*) probe location and the forces accompanying multibilayer dehydration should be considered in model calculations for probe diffusion under conditions of less than complete hydration (McCown et al., 1981; Clegg and Vaz, 1985).

MATERIALS AND METHODS

Membrane isolation and lipid preparation

Crude canine cardiac sarcolemmal membranes were isolated by the method of Jones et al. (1980). Lipids were extracted from these CSL preparations essentially by the method of Folch et al. (1957). CSL lipid preparative and analytical procedures have been described in full detail in a previous communication (Chester et al., 1987). Essentially, the lipid composition is a heterogeneous mix of phosphatidylcholine (45%), phosphatidylethanolamine (36%), phosphatidylglycerol (2%), phosphatidylserine/sphingomyelin/phosphatidic acid (11%), and phosphatidylinositol (7%). There is an additional 13 mol % endogenous cholesterol in the preparation as well. Lipid phosphorus was determined by a modification of the method of Chen et al. (1956) as described previously (Chester et al., 1987). Dioleoylphosphatidylcholine (DOPC, Avanti Biochemicals, Inc., Birmingham, AL) was demonstrated by one- and two-dimensional thin-layer chromatography to be chromatographically pure before use in diffraction studies. All organic solvents were redistilled before use.

Multilamellar vesicle preparation

CSL and DOPC lipid multilamellar vesicles for FRAP and diffraction experiments were prepared in the presence or absence of known amounts of fluorescent probe essentially by the method of Bangham et al. (1965). Lipids were dried as a thin film on glass tubes under N_2 and residual solvent removed *en vacuo* (<10 μm vacuum) for 2–4 h. A specified volume of 0.5 mM HEPES, pH 7.27, 2 mM NaCl containing rhodamine B or nisoldipine-rhodamine (Ns-R) was added to the dried lipid preparation yielding a final lipid phosphorus concentration of 3.62

μM/ml. Samples were then mixed with vortex mixer for 3 min. Brief sonication (30 s) of DOPC samples in a bath sonicator (Branson Sonic Power Co., Danbury, CT) was performed to ensure a homogeneous multiwalled vesicle suspension. Rhodamine B/lipid ratios were set initially at 1:500 and excess untrapped chromophore removed by passage down a 2-ml Sephadex G-50 column as described by Borsotto et al. (1984). This procedure involves removal of the column void volume by centrifugation for 1 min at 1,000 rpm followed by sample application and recentrifugation for 1 min at 1,000 rpm. The column effluent under these conditions contains all of the added vesicle phosphate with little change in sample volume while removing the untrapped rhodamine. In thses studies, Ns-R: lipid ratios ranged from $1:10^3$ to $1:10^5$. The $DiIC_{16}$ and NBD-PE probes (Molecular Probes, Junction City, OR) used for the determination of phospholipid diffusion coefficients were co-dried with the lipid with a constant probe/lipid ratio of $1:10^4$. All probes were assessed for purity by thin layer chromatography.

Preparation of multibilayer samples for FRAP and x-ray diffraction

The multilamellar pellets were prepared as described in detail in a previous communication (Chester et al., 1987). Briefly, 50 μl of the multilamellar vesicle preparation described above was added to lucite sedimentation cells containing either a nonfluorescent "Aclar" (Dacron, Allied Chemical Co., Morristown, NJ) or aluminum foil substrate used respectively for FRAP or diffraction measurements. The vesicles were sedimented onto the substrate at 85,000 *g* for 30 min in an SW-28 rotor (Beckman Instruments, Inc., Fullerton, CA). The normal bucket caps were then replaced with the "spin dry caps" (containing a 100 μm hole in the center) and the pelleted vesicles were spin dried at 65,000 *g* for 5 h under centrifuge vacuum. On completion of the spin-dry process, the samples were mounted and rehydrated over saturated salt solutions (Chester et al., 1987), which define specific relative humidities.

Experiments to assess the relative location of Ns-R along the bilayer normal were performed in both CSL and synthetic DOPC bilayers. Each pellet contained 250 μg of membrane phospholipid and a final ratio of Ns-R to lipid of 1:42. Drug lipid ratios were determined as a function of relative fluorescence intensity (excitation: 535 nm, emissions: 590 nm) of the supernatant and prespun samples.

Diffraction

Diffraction samples were mounted on a curved glass support and equilibrated to different humidities in a range of 66–93% in sealed brass containers at 4°C (Herbette et al., 1985). The curved multilayer specimens were exposed at 5°C to a collimated, monochromatic x-ray beam (Cuk x-rays, – 1.54 Å) from a rotating anode x-ray generator (Elliott GX-18, Marconi Avionics, Ltd., Borehamwood Hertfordshire, England). The experimental method utilizes a single Franks' mirror defining a line source where K_1 and K_2 are unresolved. CSL lipid and DOPC membrane multilayers yielded clearly defined, reproducible diffraction orders. In all cases, analyses between samples were constrained to the lowest common number of diffraction orders.

The diffraction data were recorded on both Kodak DEF-5 film (Eastman Kodak Co., Rochester, NY) and a detector (Braun Position-Sensitive model 1-D, Innovative Technologies, Inc., South Hamilton, MA). Relative intensities for the diffraction orders were obtained either by scanning x-ray films with a soft laser scanning densitometer (Zeineh model SL-2DSUV, Biomed Instruments Inc., Fullerton, CA) or by direct integration of the 1-D detector data. Data reduction (background and other geometrical corrections) for either method of data collection has been described in detail by Herbette et al. (1985). Structure factors were phased in swelling experiments (Moody, 1963) using the algorithm reported by Stamatoff and Krimm (1976).

To test whether the observed differences in the electron density profiles for DOPC multilayers in the presence and absence of Ns-R were significant (see Fig. 2), statistical analysis was done to determine the maximum amount of error in the data. After repeated cycles of data reduction, the systematic error was determined to be <5% of the integrated intensities for each of the diffraction orders. To examine the effect of the systematic error, we recalculated electron density profiles for all the data with random 5% changes (increase or decrease) in all the diffraction orders. Whereas this deliberate 5% random error in the values of the integrated intensities modulated the electron density profiles, the differences observed between the sample with and without drug were preserved and did not affect the interpretation of the data. Even a deliberate 10% random error in the integrated intensities did not affect data interpretation. Thus, based on these criteria, the changes that we have observed appear to be meaningful and are self-consistent when comparing different membrane lipid samples.

Fluorescence analyses

FRAP measurements of $DiIC_{16}$ (phospholipid) and Ns-R diffusion coefficients were performed with an excitation wavelength of 5145 A on fluorescence microscope (Ortholux II, E. Leitz, Inc., Rockleigh, NJ) equipped with a vertical illuminator, water-cooled argon laser light source (Lexel) and a galvanometric scanning mirror. The basic design and geometry of the optical system has been previously described (Koppel, 1979). The multibilayer samples were rehydrated over a well (plexiglass/glass slide assembly) containing a small bead of saturated salt solution defining a relative humidity range from 55% to 98%. All FRAP studies were carried out at 21.5°C. Samples were maintained at 4°C during equilibration intervals between analyses. The initially uniform sample fluorscence was locally depleted (or bleached) by short (40 ms) exposure to a laser beam focused by a 10X objective to a small, circularly symmetric spot. The fluorescence redistribution after photobleaching was followed with a series of 12-point scans with an attenuated monitoring beam.

The percent recovery and recovery rate were determined with a three-parameter nonlinear least squares analysis of the time decay of the fluorescence depletion monitored coincident with the position of the bleaching pulse. To determine the bleach spot size, *w*, used to calculate the diffusion coefficients from recovery rates, the immediate post-bleach intensity profile was reconstructed (by empirically extrapolating the fluorescence traces measured at each position back to time zero) and fit to an assumed Gaussian profile (Koppel, 1979).

Modeling of the interbilayer water space

To model the interbilayer water space, a step-function equivalent profile, with step widths constrained to 9-Å resolution limits of the experimental data, was fitted to the continuous experimental CSL electron density profile structure. The step-function equivalent was Fourier transformed once to obtain a continuous structure factor function which was truncated at the resolution limits of the experiment. When the calculated profile structure and its intensity function correlated well with the experimental profile structure (see Fig. 4 *A*) and intensity data, calculations were terminated (Herbette et al., 1985).

At 66% relative humidity, the interbilayer water space was determined to be ~5 Å using the step-function plot. The phosphate to phosphate distance across the water space ($D - D_{p-p}$) is 12 Å at this relative humidity and, therefore, ~3–4 Å outside the phosphate peaks could be ascribed to the edge of the headgroups (see Fig. 4 *A*). Since the

TABLE 1 Structure factors for cardiac sarcolemmal lipid multilayers at distinct unit cell repeat distances

64 Å (h = 1→5)	59 Å (h = 1→5)	58 Å (h = 1→4)	56 Å (h = 1→6)
1 = −0.695	1 = −0.830	1 = −0.865	1 = −0.875
2 = −0.585	2 = −0.405	2 = −0.155	2 = −0.105
3 = +0.215	3 = +0.330	3 = +0.205	3 = +0.050
4 = 0.0	4 = −0.230	4 = −0.370	4 = −0.600
5 = −0.275	5 = −0.130	5 = 0.0	5 = +0.160
6 = 0.0	6 = 0.0	6 = 0.0	6 = −0.195

distance between intrabilayer phosphate headgroups (D_{p-p}) remained constant throughout the hydration series (evaluated using constant resolution limits), we extrapolated values for the extent of the interbilayer water space at the other relative humidities based on the modeling results at 66% as follows: $D_w = D - (D_{p-p} + 7$ Å), where D = unit cell repeat distance; D_{p-p} = distance between phosphate peaks; 7 Å represents the added extent of the headgroups into the interbilayer region between phosphate peaks.

The structure factors for the CSL multilayers at distinct unit cell repeat distances are presented in Table 1.

RESULTS AND DISCUSSION

Fig. 1 illustrates the probes and their probable bilayer locations based on their physical and chemical properties as well as recent diffraction data on DHPs in model and native bilayer systems. The size and calculated van der Waal volumes of the probes are: free rhodamine (molecular weight 479) is 228 Å^3; $DiIC_{16}$ (molecular weight 880) is 872 Å^3; and Ns-R (molecular weight = 1,070) is 788 Å^3. The free rhodamine is presumed to be located in the interbilayer water space since studies by Loew and coworkers (1986) indicate that some charged rhodamines (e.g., rhodamine 123), do not appear to penetrate the membrane bilayer. This location is further supported by the diffusion data to be shown below. The $DiIC_{16}$ probe used to assess phospholipid diffusion was oriented with the acyl chains completely embedded in the bilayer hydrocarbon region and the charged amine at the level of the hydrocarbon core/water interface. The DHP has been shown by diffraction studies to have an equilibrium position within the first few methylene segments (Herbette et al., 1986; Mason et al., 1989*b*). Lastly, as will be discussed below, we have determined that the Ns-R complex appears to be located with the rhodamine and DHP moieties in the aqueous and interfacial regions, respectively. Since, in our previous studies, we observed significant differences in diffusional dynamics between the two membrane-bound probes (Ns-R and $DiIC_{16}$), we reasoned that relative probe location and molecular distribution along the bilayer normal could strongly impact their diffusional characteristics.

Preliminary diffraction results on the Ns-R complex location in DOPC membranes are presented in Fig. 2. This membrane system has been used previously to determine the time-averaged location of DHP ligands (Mason et al., 1989*a*). Lissamine rhodamine has two sulfur substituents to the chromophores heterocyclic ring structure. Since these should scatter with an intensity similar to that of phosphate, it should be possible to identify its location along the bilayer normal. As illustrated by the stippled difference profile for Ns-R versus control membranes in Fig. 2, there is added relative electron density to

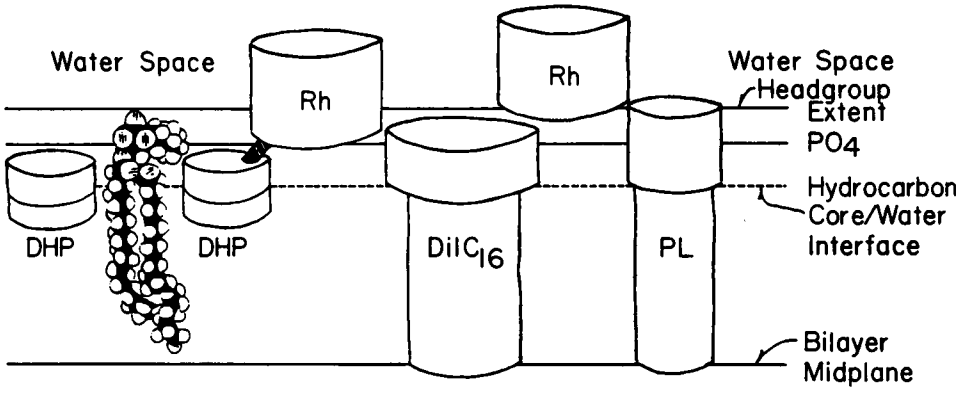

FIGURE 1 "Oil can" model describing the relative locations within a membrane monolayer of DHP, Ns-R, $DiIc_{16}$, free rhodamine, and phospholipid. This model depicts these ligands in either predicted ($DiIC_{16}$, free rhodamine) or determined locations (Ns-R, DHP, and phospholipid) as well as maintains the relative size relationships from van der Waals volume calculations. The interaction forces exerted on each of these molecules could be somewhat different. $DiIC_{16}$ interacts with frictional drag forces at the bilayer midplane and at the glycerol backbone region of the bilayer. Ns-R has no interactions in the bilayer midplane but has substantial interactions in the headgroup region which would be affected strongly by interbilayer forces (i.e., electrostatic, hydration, steric). Free rhodamine, while large, does not appear to interact within the bilayer and, as such, would not be expected to experience the same set of hydration forces detected by the membrane bound ligands. DHP, on the other hand, sits at the hydrocarbon core/water interface and appears to have little interaction with the headgroups or bilayer midplane.

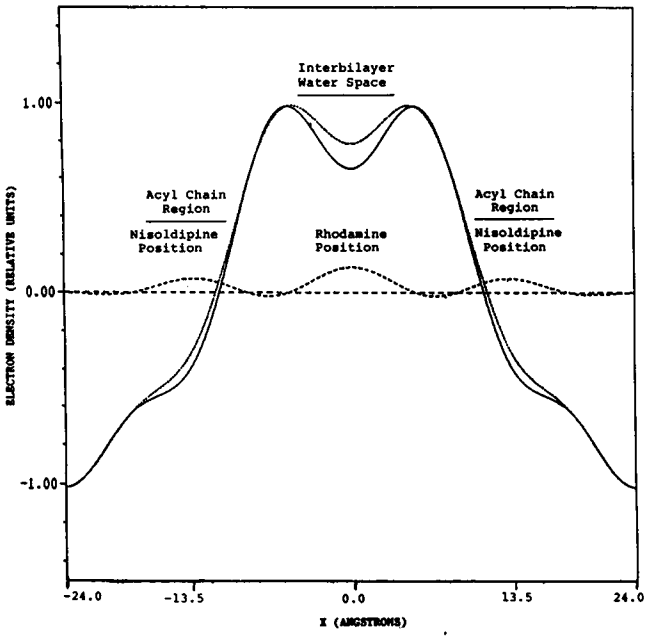

FIGURE 2 One-dimensional electron density profile for a DOPC lipid bilayer at 34% relative humidity (relative electron density vs. angstroms across the bilayer). This figure shows the DOPC membrane in the presence (· · · · ·) and absence (----) of Ns-R along with the difference profile (- - - -). These data were calculated at a resolution of 7 Å. The two peaks of electron density correspond to the phospholipid headgroup; the electron density minima at the edges of the figure correspond to the terminal methyl groups at the bilayer center. The positive changes in electron density are attributed to the presence of the Ns-R complex (see Results and Discussion).

both the water space and the region corresponding to the hydrocarbon core/water interface. We have attributed the added electron density at the interface to the DHP moiety of the Ns-R complex. This location, as discussed above, is consistent with that observed for other DHPs. We have attributed the added electron density in the water space to that of the rhodamine moiety of the Ns-R complex. Since lissamine would be a zwitterion at physiological pH (charged amino and sulfate groups), this molecule is not likely to be found in the center of the bilayer. As well, the diffusion coefficient data for free rhodamine is consistent with diffusion in the aqueous phase between the bilayers (discussed below) and, again, argues for rhodamines location in the interbilayer water space of the membrane profile structure.

Interestingly, the distance between the center of mass of the increase in electron density attributed to the rhodamine and DHP moieties is ~13 Å. In evaluating the structure of the Ns-R complex, an extended, all-*trans* configuration of the aliphatic chain linking the DHP and rhodamine moieties would give an approximate distance of 22 Å. Hence, as would be anticipated, gauche rotomers would be allowed in the 11-methylene segment region between the end of the DHP 5'-carboxylate substituent and the sulfonyl linkage to the rhodamine chromophore. In our previous communication, data was presented demonstrating that shorter methylene segment lengths result in decreased competitive displacement of other DHP from their specific binding site on the DHP receptor (Chester et al., 1987). These diffraction results would suggest a rationale for this effect in that shortening the methylene segment to two carbons would cause the DHP moiety to be displaced from the bilayer interfacial region and, hence, render the DHP less capable of binding into the receptor binding domain.

We have used the multipoint FRAP analysis, described by Koppel (1979), to determine the diffusion coefficients of free rhodamine compared with the active DHP calcium channel antagonist (Ns-R) and phospholipid ($DiIC_{16}$) in purified CSL lipid multibilayers. Since DHP drug molecules with intrinsic fluorescence are not available for diffusional dynamic studies, we are attempting to further evaluate our previous Ns-R complex diffusion data by studying the relative differences in diffusion between free rhodamine and the membrane bound, rhodamine tagged ligand. At present, it is considered that small molecules of similar size to phospholipid would have diffusion coefficients essentially the same as phospholipid (Vaz et al., 1985). While this may be true for the completely hydrated bilayers, our data clearly show differences in diffusion for molecules of similar size as a function of relative bilayer hydration.

The diffusion coefficient data collected for these studies is summarized in Fig. 3 (NBD-PE was also used as a phospholipid probe and yielded similar diffusion rates, within experimental error, as the $DiIC_{16}$). At the lowest partial hydration measured, 55%, free rhodamine diffusion ($4.4 \pm 0.3 \times 10^{-9}$ cm^2/s) was over an order of magnitude faster than Ns-R ($2.3 \pm 0.3 \times 10^{-10}$ cm^2/s). As observed previously (Chester et al., 1987), $DiIC_{16}$ diffusion ($6.8 \pm 1.0 \times 10^{-10}$ cm^2/s) was approximately three times faster than that observed for the Ns-R complex and six times slower than that of free rhodamine (Fig. 3 *b*). As the bilayers were successively hydrated from 55% to 93% relative humidity, the diffusion coefficients for free rhodamine diffusion increased in a linear fashion with significantly faster diffusion values than that observed for both Ns-R and $DiIC_{16}$ (Fig. 3).

As discussed above, the relative differences in diffusion could be related to differential effects of the various inter- and intramembrane forces accompanying partial bilayer hydration as a function of differences in probe location (see Fig. 1). For example, if free rhodamine is located primarily in the interbilayer water space, its diffusion in the water space would be expected to be substantially less constrained by intrabilayer forces resultant from partial

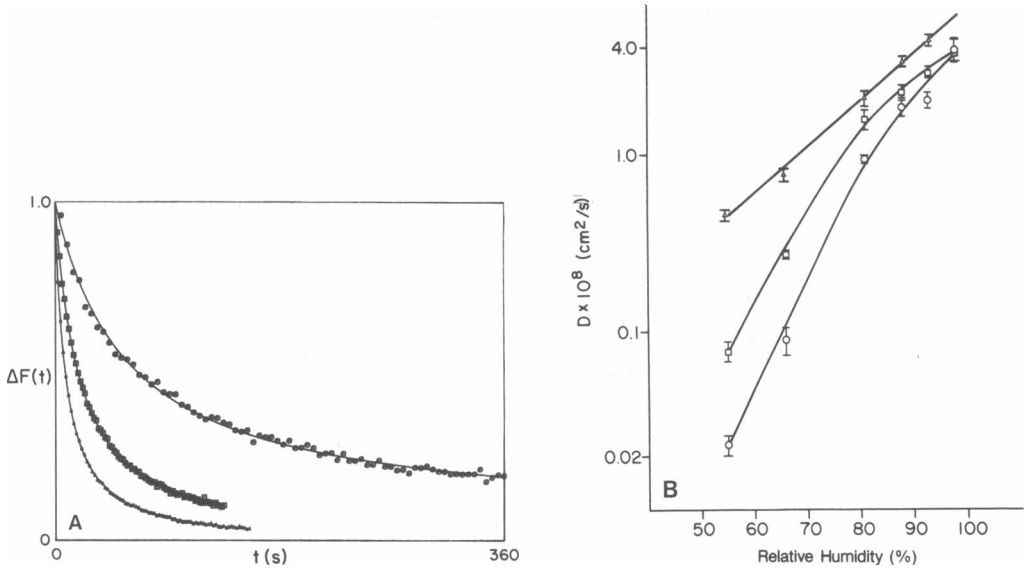

FIGURE 3 (*A*) FRAP data showing the recovery in sample fluorescence as a function of time for the point coincident with the bleach spot. A three-parameter least squares fit was drawn through these data points as described in Materials and Methods. These data were collected from CSL lipid bilayers at 21.5°C and 66% relative bilayer hydration to demonstrate the significant difference in rates of recovery for Ns-R (⊙), $DiIC_{16}$ (▣), and free rhodamine (▲). (*B*) Log plot of lateral diffusion coefficients of the three probes as a function of relative humidity in CSL lipid bilayers at 21.5°C. This plot highlights the effects of relative bilayer hydration on the diffusional rates for Ns-R (○), $DiIC_{16}$ (□), and free rhodamine (△). Plots for $DiIC_{16}$ and Ns-R are reproduced from Chester et al. (1987) such that a comparison can be made between free rhodamine and membrane bound Ns-R diffusion. (Data were also regenerated as controls for this study).

dehydration. When free rhodamine diffusion is evaluated as a function of interbilayer water space (see Fig. 5), it becomes even clearer that partial dehydration effects on its diffusion differ substantially from that observed for phospholipid and Ns-R below the transition from free to bound water (*arrow* in Fig. 5).

The free rhodamine diffusion coefficient measured in this system at the highest relative humidity (0.98) is at least two orders of magnitude slower than that expected for pure aqueous phase diffusion (Figs. 3 and 5). These data would suggest that there are electrostatic interactions between the charged rhodamine and the bilayer. The change of slope for free rhodamine diffusion below the free to bound water transition (*arrow*) would be indicative of interbilayer steric and structured water constraints as the phospholipid headgroups become more closely apposed.

We have used low-angle X-ray diffraction to model the cardiac sarcolemmal (CSL) interbilayer water space (Fig. 4 *A*) and plotted these distances as a function of applied pressures calculated by the equation of McIntosh et al. (1987) described in Materials and Methods (Fig. 4 *B*). Modeling results show that while the distance between phosphate peaks (D_{p-p}) is invariable throughout the hydration series, the interbilayer water space increases 9 Å, from ~4 Å at 55% relative humidity to 13 Å at 98% relative humidity. These measured changes (see Fig. 4 *B*) are larger than that observed for model membrane systems (White and King, 1985; McIntosh and Simon, 1986; McIntosh et al., 1987). We attribute this to the heterogenous composition of the CSL lipid bilayers and the presence of cholesterol (Jendrasiak and Hasty, 1974).

Lundberg and co-workers (1978) observed a transition point between free and bound water in model membrane systems at 84% relative humidity. When plotting the lateral diffusion coefficients of the probes as a function of interbilayer water space a similar transition could be identified in the region of ~87% relative humidity (Fig. 5). While the plot is clearly curvilinear, fitting a straight line to the upper and lower portions of the curve intersect around 87% relative humidity, suggesting a broad transition at about this region. A broad transition would be expected for this membrane due primarily to lipid heterogeneity (see Materials and Methods). This conclusion is supported by the reasonably wide disparity in waters of hydration reported by Jendrasiak and Hasty (1974) as a function of lipid class, acyl chain saturation, and presence of cholesterol.

As the bilayers are dehydrated, the decrease in distance between apposing bilayers is accompanied by increasing repulsive forces including electrostatic (Israelachvili and Adams, 1978), hydration (McIntosh and Simon, 1986, Parsegian et al., 1979), and steric (McIntosh et al., 1987).

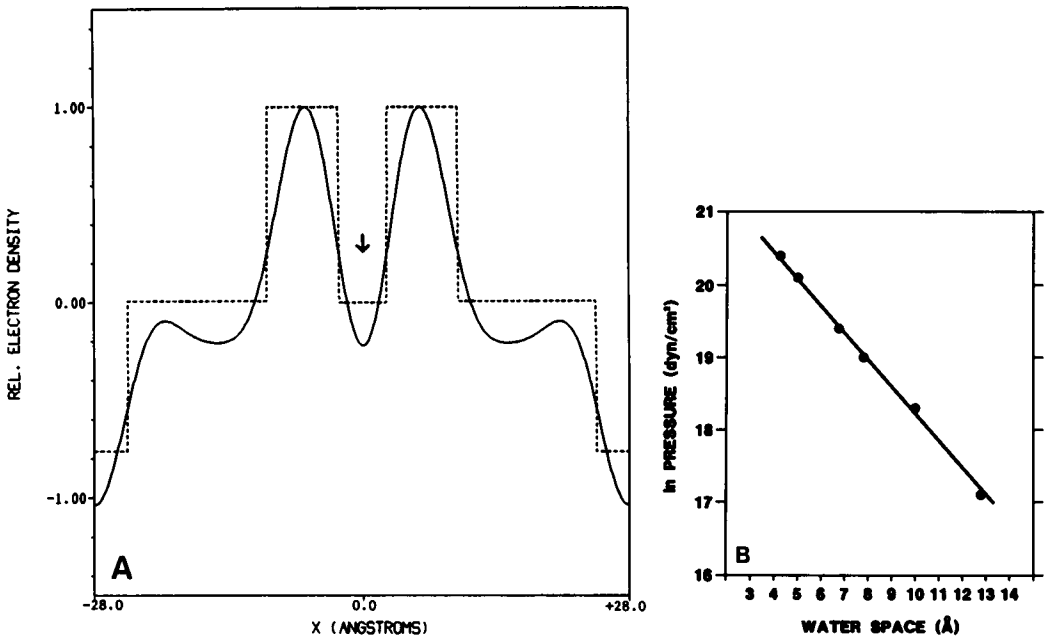

FIGURE 4 (*A*) One-dimensional electron density profile for a CSL lipid bilayer at 66% relative humidity (relative electron density vs. angströms across the membrane bilayer). The experimental electron density profile is indicated by the *solid line;* the *dashed line* represents the real space-step function model. Step-function modeling of the bilayer indicated a 5-Å interbilayer water space at this relative humidity. The location of the interbilayer water space region is shown by the *arrow*. The unit cell repeat distance of this bilayer is 56 Å. (*B*) The change in interbilayer water space of CSL lipid multibilayers as a function of the natural log of applied pressure (dyn/cm^2). Applied pressure as a function of vapor pressure was calculated according to the equations of McIntosh et al. (1987): $P = RT/V_w \ln (P_i/P_o)$, where R is the molar gas constant, T is temperature (°K), V_w is the molar volume of water (18 cm^3/mol), and P_i/P_o is the relative vapor pressure. As applied pressure increases, there is a nonlinear decrease in the interbilayer water space. The unit cell repeat distances as a function of relative humidity were measured as follows: 64 Å (0.98); 61 Å (0.93); 59 Å (0.87); 58 Å (0.81); 56 Å (0.66); 55 Å (0.55).

The combined effects of hydration pressure (resulting from the work required to remove polarized water molecules from between bilayers) and steric interactions between phospholipid headgroups have been recently examined as a function of interbilayer water space by McIntosh et al. (1987). Decreases in the water space result in a significant increase in energy between apposing bilayers expressed as a function of applied pressure (2.7×10^7 dyn/cm^2 up to 6.5×10^8 dyn/cm^2, see Fig. 4 *B*). In their analyses, McIntosh and co-workers suggest that the effect of hydration pressure predominates at applied pressures less than of $\sim 2 \times 10^7$ dyn/cm^2 while steric forces predominate at pressures above $\sim 5 \times 10^8$ dyn/cm^2. Intrabilayer forces, e.g. reduction in the surface area available per lipid molecule as water molecules are removed would also be expected to impact diffusion of these probes as a function of relative humidity (Small, 1967; Parsegian et al., 1979). This effect has previously been shown to significantly reduce the rate of lateral diffusion of the phospholipid probe NBD-PE (McCown et al., 1981).

Decreasing the relative humidity of the multilayers impacts probe diffusion both within the interbilayer water space and at the bilayer surface, as illustrated in Fig. 5. This is indicated by the sharp change in $DiIC_{16}$ and Ns-R diffusion coefficient curves as repulsive interactions are increased at decreased bilayer relative humidity. The relatively mild slope change for free rhodamine diffusion below 87% relative humidity suggests a differential affect of these forces on probe diffusion in the interbilayer water space. We have interpreted these differences to be related to the relative degrees of freedom for probes, like rhodamine, diffusing in the interbilayer water space. As well, we anticipate that probe diffusion in the water space would be less compromised by intrabilayer condensation forces as previously described. These data highlight the need to consider more thoroughly intrabilayer and interbilayer forces in model calculations for probe diffusion under conditions of less than complete hydration.

At the highest relative humidity (0.98), both Ns-R and phospholipid analogs diffuse at similar rates (3.8×10^{-8} cm^2/s) consistent with the rates of diffusion for probes in other membrane systems and free volume model calculations (Wu et al., 1977; Galla et al., 1979; Vaz et al., 1985; Eisenger and Halperin, 1986). However, free rhodamine under these same conditions diffuses significantly faster,

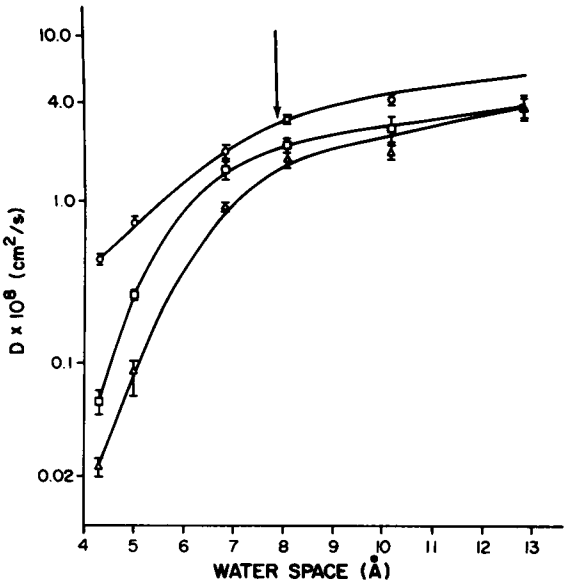

FIGURE 5 Lateral diffusion coefficients as a function of interbilayer water space based on step-function modeling of the CSL bilayer electron density profile (see Materials and Methods). The data collected for lateral diffusion (Fig. 2) were plotted against the water space determined for each applied pressure (Fig. 3*B*). The probes measured are free rhodamine (○), $DiIC_{16}$ (□), and Ns-R (△).

at ~6.5 × 10^{-8} cm^2/s (see Fig. 3 *B*). The observation that Ns-R and phospholipids diffuse at similar rates, while "free" rhodamine diffuses yet faster, suggests that the Ns-R complex diffusion is primarily rate-limited by the membrane-bound nisoldipine. As such, we interpret the Ns-R diffusion to represent a lower limit of the DHP's absolute diffusion under conditions of maximum bilayer hydration.

We thank Dr. D. E. Triggle for his gracious gift of the Ns-R compound used in these studies; Drs. L. G. Herbette and D. E. Koppel for the use of their diffraction and FRAP instrumentation and important discussions pertaining to the interpretation of the data and Peter Febroriello for assistance with the FRAP computer software and hardware: and Dr. David G. Rhodes for his invaluable insight during discussions pertaining to these studies. The diffraction aspect of this work was carried out with the assistance of the staff of the Biomolecular Structure Analysis Center at the University of Connecticut Health Center. The graphics analyses were performed using CHEMX software, a package designed and distributed by Chemical Design Ltd., Oxford, England.

This work was supported by National Institutes of Health trainee grant HL-07240 and research grants HL-33026 and GM-23585, a grant from the Whitaker Foundation, a Health Center Research Advisory Committee grant, and a gift from the Patterson Trust Foundation and RJR Nabisco, Inc.

Received for publication 19 April 1989 and in final form 15 August 1989.

REFERENCES

Bangham, A. D., M. M. Standish, and J. C. Watkins. 1965. Diffusion of univalent ions across the lamellae of swollen phospholipids. *J. Mol. Biol.* 13:238–252.

Borsotto, M., R. I. Norman, M. Fosset and M. Lazdunski. 1984. Solubilization of the nitrendipine receptor from skeletal muscle transverse tubule membranes: interaction with specific inhibitors of the voltage-dependent Ca^{2+} channel. *Eur. J. Biochem.* 142:449–455.

Chen, P. S., Jr., T. Y. Toribara, and H. Warner. 1956. Microdetermination of phosphorous. *Anal. Chem.* 28:1756–1758.

Chester, D. W., L. G. Herbette, R. P. Mason, A. F. Joslyn, D. J. Triggle, and D. E. Koppel. 1987. Diffusion of dihydropyridine calcium channel antagonists in cardiac sarcolemmal lipid multibilayers. *Biophys. J.* 52:1021–1030.

Clegg, R. M., and W. L. C. Vaz. 1985. Translational diffusion of proteins and lipids in artificial lipid bilayer membranes: a comparison of experiment with theory. *In* Progress in Protein–Lipid Interactions. Elsevier Science Publishers B.V., Amsterdam. 173–229.

Colvin, R. A., T. F. Ashavaid, and L. G. Herbette. 1985. Structure-function studies of canine cardiac sarcolemmal membranes. I. Estimation of receptor site densities. *Biochim Biophys. Acta.* 812:601–608.

Eisenger, J. and B. I. Halperin. 1986. Effects of spatial variation in membrane diffusibility and solubility on the lateral transport of membrane components. *Biophys. J.* 50:513–521.

Folch, J., M. Lees, and G. A. Sloane-Stanley. 1957. A simple method for the isolation and purification of total lipids from animal tissues. *J. Biol. Chem.* 226:447–509.

Frenzel, J., K. Arnold, and P. Nuhn. 1978. Calorimetric, ^{13}C-NMR and ^{31}P-NMR studies on the interaction of some phenothiazine derivatives with dipalmitoyl phosphatidylcholine model membranes. *Biochim. Biophys. Acta.* 507:185–197.

Galla, H.-J., U. T. Hartmann, and E. Sackman. 1979. On two-dimensional random walk in lipid bilayers and fluid pathways in biomembranes. *J. Membr. Biol.* 48:215–236.

Giraudat, J., M. Dennis, T. Heidmann, P. Y. Haumont, R. Lederer, and J. P. Changeux. 1987. Structure of the high-affinity site for noncompetitive blockers of the acetylcholine receptor: [^3H]chlorpromazine labels homologous residues in the beta and delta chains. *Biochemistry.* 26:2410–2418.

Herbette, L. G., T. MacAlister, T. F. Ashovaid, and R. A. Colvin. 1985. Structure-function studies of canine cardiac sarcolemmal membranes. II. Structural organization of the sarcolemmal membranes as determined by electron microscopy and lamellar x-ray diffraction. *Biochim. Biophys. Acta.* 812:609–623.

Herbette, L. G., D. W. Chester, and D. G. Rhodes. 1986. Structural analysis of drug molecules in biological membranes. *Biophys. J.* 49:91–93.

Israelachvili, J. N., S. Marcelja, and R. G. Horn. 1980. Physical principles of membrane organization. *Q. Rev. Biophys.* 13:121–200.

Janis, R. A., P. J. Silver, and D. J. Triggle. 1987. Drug action and cellular calcium regulation. *Adv. Drug Res.* 16:309–591.

Jendrasiak, G. L., and J. H. Hasty. 1974. The hydration of phospholipids. *Biochim. Biophys. Acta.* 337:79–91.

Jones, L. R., S. W. Maddock, and H. R. Besch. 1980. Unmasking effects of alamethacin on the (Na/K^+)-ATPase, β-adrenergic receptor-coupled adenylate cyclase and cAMP-dependent protein kinase activities in cardiac sarcolemmal vesicles. *J. Biol. Chem.* 255:9971–9980.

Kobilka, B. K., P. S. Kobilka, K. Daniel, J. W. Regan, M. G. Caron, and

R. J. Lefkowitz. 1988. Chimeric α-2-β-2 adrenergic receptors: delineation of domains involved in effector coupling and ligand binding specificity. *Science (Wash. DC).* 240:1310–1316.

Koppel, D. E. 1979. Fluorescence redistribution after photobleaching: a new multipoint analysis of membrane translational dynamics. *Biophys. J.* 28:281–291.

Loew, L. M., B. Ehrenberg, E. Fluhler, M.-D. Wei, and V. Burnham. 1986. A search for nerstian dyes to measure membrane potential in individual cells. *Biophys. J.* 49, 308*a*. (Abstr.)

Lundberg, B., E. Svens, and S. Ekman. 1978. The hydration of phospholipid–cholesterol complexes. *Chem. Phys. Lipids.* 22:285–292.

Mason, R. P., S. E. Campbell, S. D. Wang, and L. G. Herbette, 1989*a*. A comparison of location and binding for the positively charged 1,4-dihydropyridine calcium channel antagonist amlodipine with uncharged drugs of this class in cardiac membranes. *Mol. Pharmacol.* In press.

Mason, R. P., G. E. Gonye, D. W. Chester, and L. G. Herbette. 1989*b*). Partitioning and location of Bay K 8644, a 1,4-dihydropyridine calcium channel agonist, in model and biological lipid membranes. *Biophys. J.* 55:769–778.

McCown, J. T., E. Evans, S. Diehl, and H. C. Wiles. 1981. Degree of hydration and lateral diffusion in phospholipid multibilayers. *Biochemistry.* 20:3134–3138.

McIntosh, T. J., and S. A. Simon. 1986. Hydration force and bilayer deformation: a reevaluation. *Biochemistry.* 25:4058–4066.

McIntosh, T. J., A. D. Magid, and S. A. Simon. 1987. Steric repulsion between phosphatidylcholine bilayers. *Biochemistry.* 26:7325–7332.

Moody, M. F. 1963. X-ray diffraction pattern of nerve myelin: a method for determining the phases. *Science (Wash. DC).* 142:1173–1174.

Parsegian, V. A., N. Fuller, and R. P. Rand. 1979. Measured work of deformation and repulsion of lecithin bilayers. *Proc. Natl. Acad. Sci. USA.* 76:2750–2754.

Rhodes, D. G., J. G. Sarmiento, and L. G. Herbette. 1985. Kinetics of binding of membrane-active drugs to receptor sites: diffusion limited rates for a membrane bilayer approach of 1,4-dihydropyridine calcium channel antagonist to their active site. *Mol. Pharmacol.* 27:612–623.

Small, D. M. 1967. Phase equilibria and structure of dry and hydrated egg lecithin. *J. Lipid Res.* 8:551–557.

Stamatoft, J. B., and S. Kriman. 1976. Phase determination of x-ray reflections for membrane-type systems with constant fluid density. *Biophys. J.* 16:503–516.

Tanabe, T., H. Takeshima, A. Mikami, V. Flockerzi, H. Takahashi, K. Kangawa, M. Kojima, H. Matsuo, T. Hirose, and S. Numa. 1987. Primary structure of the receptor for calcium channel blockers from skeletal muscle. *Nature (Lond.)* 328:313–318.

Vaz, W. L. C., R. M. Clegg, and D. Hallman. 1985. Translational diffusion of lipids in liquid crystalline phase phosphatidylcholine multibilayers: a comparison of experiment with theory. *Biochemistry.* 24:781–786.

White, S. H., and G. I. King. 1985. Molecular packing and area compressibility of lipid bilayers. *Proc. Natl. Acad. Sci. USA.* 82:6532–6536.

Wu, E.-S, K. Jacobson, and D. Papahadjopoulos. 1977. Lateral diffusion in phospholipid multilayers measured by fluorescence recovery after photobleaching. *Biochemistry.* 16:3936–3941.